Experimental investigation on effect of partial flexibility at low aspect ratio airfoil – Part I: Installation on suction surface

Mustafa Serdar Genç[1,*], *Halil Hakan* Açıkel[1], *Kemal* Koca[1]

[1]Wind Engineering and Aerodynamic Research Center, Department of Energy Systems Engineering, Erciyes University, Kayseri, TURKEY

Abstract. Effects of flexible membrane mounted over suction surface of NACA 4412 airfoil were experimentally investigated at Reynolds number of $5x10^4$ and low aspect ratio (AR=1) in this paper. The smoke-wire visualization method has been performed for flow visualization to demonstrate flow phenomena as laminar separation bubble (LSB), leading edge separation at z/c=0.4 and tip vortices at z/c=0.1. Values of velocity, Reynolds stress and turbulence statistics were measured by means of a constant temperature anemometer (CTA) system. Results of smoke-wire experiment revealed that size and height of LSB formed along z/c=0.4 at lower angles of attack such as α=8° was mitigated. Moreover, stall phenomenon as a result of boundary layer separation was apparently postponed at higher angles of attack. Velocity value was increased, whereas values of Reynold stress and turbulent kinetic energy was decreased with reduction of amount of fluctuations in flow. Consequently, using flexible membrane over suction surface of airfoil allowed the LSB to be mitigated or extinguished, resulting in exhibition of more stable flow characteristics.

1 Introduction

Micro Air Vehicles (MAVs) mostly run under Reynolds (Re) number of $1x10^5$ [1-4]. In this flow regime, accurately determination of LSB and prediction of transition phenomenon inside LSB are obligatory. Because, these two flow phenomena can occur the suction surface of airfoils, resulting in the abrupt reduction at aerodynamic performance [4-9] because of low Reynolds number airfoil drag generally depends upon position of transition (essentially in a short LSB) as a function of angle of attack. Until now, aerodynamic researchers have carried out many experimental and numerical methods to investigate and observe the location of LSB and transition. Moreover, they have applied few control techniques such as acoustic excitation [10-11], leading-edge slats [12], vortex generators [13], roughness material [14-15] since they want to eliminate LSB and hinder the deterioration of aerodynamic efficiency.

In addition to these control techniques, the bio-inspired design such as flexible membrane for MAVs have been started to gain interests and reputations recently. Maximum stall angle and lift coefficient as well as vehicle agility can be ensured with the use of flexible membrane wings for MAVs [16-32].

In this study, the experiments containing smoke-wire and hot-wire measurements are performed for partial flexible NACA 4412 wing, which has aspect ratio (AR) of 1, at Reynolds number of $5x10^5$ and angle of attack (α) of 8º, 12º, 20º. In addition, the results of partial flexible airfoil are compared with the results of our former study [19] to see how flexible membrane affects the aerodynamic performance.

2 Experimental Rigs

The wing airfoil has 18 cm chord and 18 cm span length. The experiments are carried out wind tunnel where the free stream turbulence intensity is quite low. The detailed information with regards to wind tunnel has been ensured in Ref. [9, 14-15]. 3D printer has been utilized for manufacturing process of partial flexible wing. As shown in the Figure 1, membrane is mounted between x/c=0.2 and x/c=0.7 since LSB and separation, which affects the aerodynamic performance negatively, occurs between these points. As the technical features of flexible membrane, latex rubber sheet which has Young's modulus (E) of 2.2 MPa and density (ρ_m) of 1 g/cm^3 [19] is 0.2 mm. It is adhered onto rigid skeleton of airfoil with double side tape.

* Corresponding author: musgenc@erciyes.edu.tr

As demonstrated in the Figure 2, measurements are conducted along z/c=0.1 and z/c=0.4. The experiments along z/c=0.1 ensures tip vortices and their effects very well, whilst LSB and flow separation are especially obtained from experiments along z/c= 0.4.

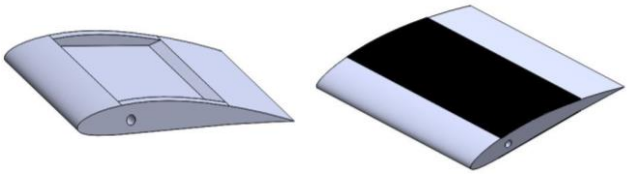

Fig. 1. The fabricating process of partial flexible airfoil [19].

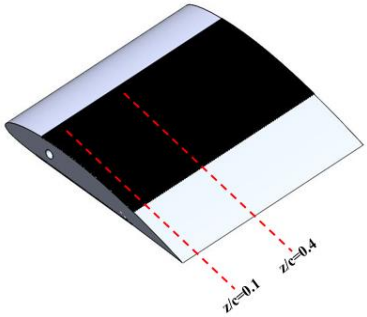

Fig. 2. Sketch of the measurements line.

2.1 Flow visualization system

Tip vortices occurred at tip of NACA 4412 and flow separation, LSB formed over suction surface have been visualized by means of smoke-wire experiment. The essential components of this technique are electrical resistive heating, 0.03 mm diameter steel wire, an oil mixture, a compact camera (the Canon EOS-D1100 type), and two or three halogen lambs. The arrangement of smoke-wire technique, the most prevalent of which has been performed by Koca et al. [9] and Genç et al. [14-15], can be found in mentioned References.

2.2 Velocity Distribution and Turbulence Statistics

In addition to the smoke-wire experiment, hot-wire experiment has been performed to investigate flow velocity, turbulence intensity and Reynolds stresses. Two-dimensional wire probe has been functioned with utilizing of a constant temperature anemometer (CTA) at the over and wake of airfoil (at the distance of 1c and 2c). The probe has been run with the intervals of x/c=0.1 along the chord-wise via traverse system. 20480 data have been obtained with a sample rate of 2 kHz at selected x/c. Furthermore, the reference velocity probe has been used for probe calibration and the calibration error has been measured about ±1%.

Regarding equations, averages of u and v velocity components, the velocity standard deviation, the turbulence intensity and Reynolds stresses have been calculated with Equation (1), Equation (2), Equation (3), Equation (4), respectively as follows:

$$U_{mean} = \frac{1}{N}\sum_{i}^{N} U_i \tag{1}$$

$$U_{rms} = \left(\frac{1}{N-1}\sum_{i}^{N}\left(U_i - U_{mean}\right)^2\right)^{0.5} \tag{2}$$

$$Tu = \frac{U_{rms}}{U_{mean}} \tag{3}$$

$$\overline{u'v'} = \frac{1}{N}\sum_{i}^{N}(U_i - U_{mean})(V_i - V_{mean}) \tag{4}$$

3 Results

3.1 Smoke-wire results

It is observed from Figure 3(a) that the flow separates (referred as **S** with green arrow) from x/c=0.2 and almost reattaches (referred as **R** with green arrow) to x/c=0.8, resulting in formation of long separation bubble. On the other hand, it is clearly seen that size of LSB is reduced with the using of partial flexible membrane. Because LSB is occurred between x/c=0.2 and x/c=0.5. Flexible membrane causes the flow to gain momentum and this momentum transfer ensures the separated flow to reattaches at x/c=0.5. Therefore, the reduction of 50% (0.3c) at size of LSB is observed.

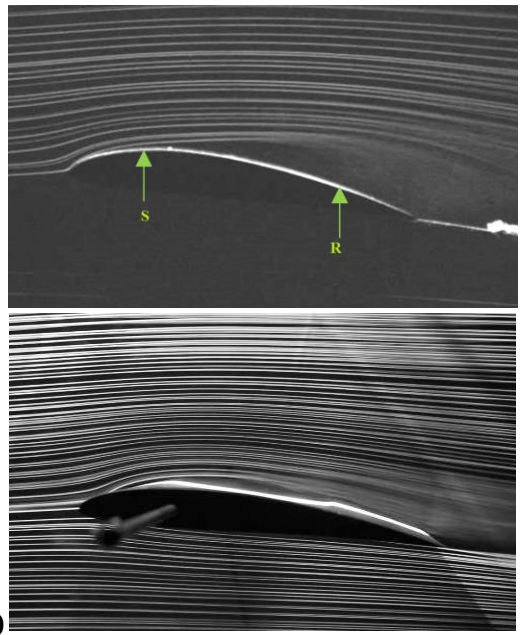

Fig. 3. Smoke-wire results for Re=5x10^4, α=8º and z/s=0.4 a) uncontrolled case [19], b) partial flexible airfoil.

Figure 4 and Figure 5 have indicated tip-vortices formation at α=12° and at α=20° for both uncontrolled case and partially flexible airfoil, respectively. It has been clearly noticed from the figures that size of tip-vortices has decreased with using of membrane material. Moreover, the wake region of partially flexible skinned airfoil has narrower than the wake region of uncontrolled case, meaning that airfoil drag force and coefficient decreased. Thereby, utilizing the membrane material over suction surface of the airfoil causes aerodynamic performance to increase.

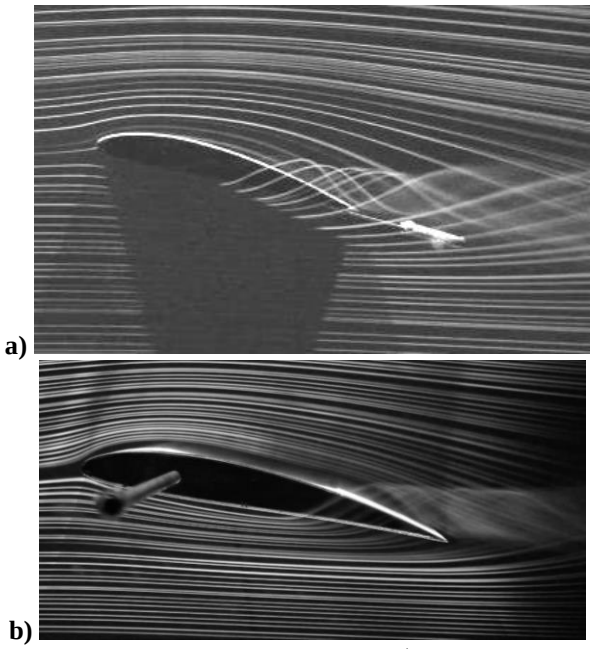

Fig. 4. Smoke wire results for Re=5x10^4, α=12º and z/s=0.1 a) uncontrolled case, b) partial flexible airfoil.

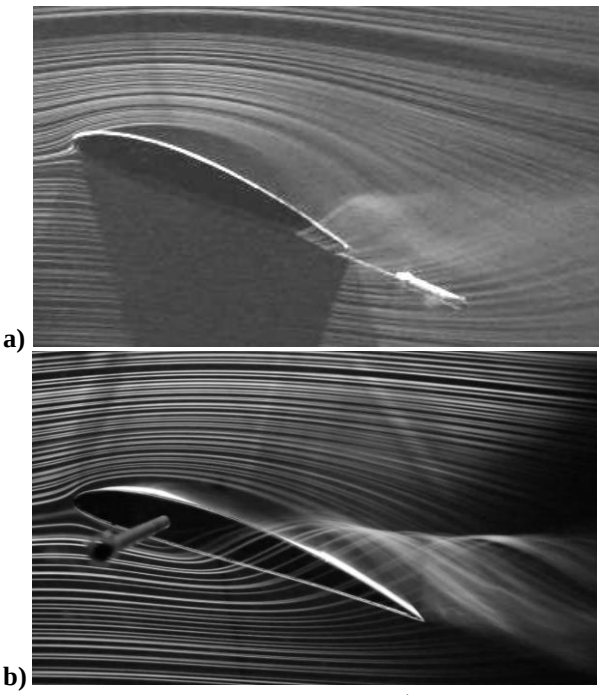

Fig. 5. Smoke wire results for Re=5x10^4, α=20º and z/s=0.1 a) uncontrolled case, b) partial flexible airfoil.

3.2 Velocity Distribution and Turbulence Statistics

Velocity measurement and turbulence statistics including turbulence intensity and Reynolds stresses at Re=5x10^4 and α=8º are investigated for better understanding of using of partial flexible membrane over suction surface of airfoil. Uncontrolled case of velocity measurement (in Figure 6(a)) reveal that flow separation which is caused by adverse pressure gradient (APG) occurs between x/c=0.4 and x/c=0.5 and lower velocity region at leading-edge is observed. But, as seen in Figure 6(b), amount of velocity over suction surface is apparently increased via flexible membrane, causing the increase of lift and aerodynamic performance. Furthermore, separated flow does not nearly occur over suction surface and energized flow by using flexible membrane causes the separated shear layer to approach the surface of airfoil.

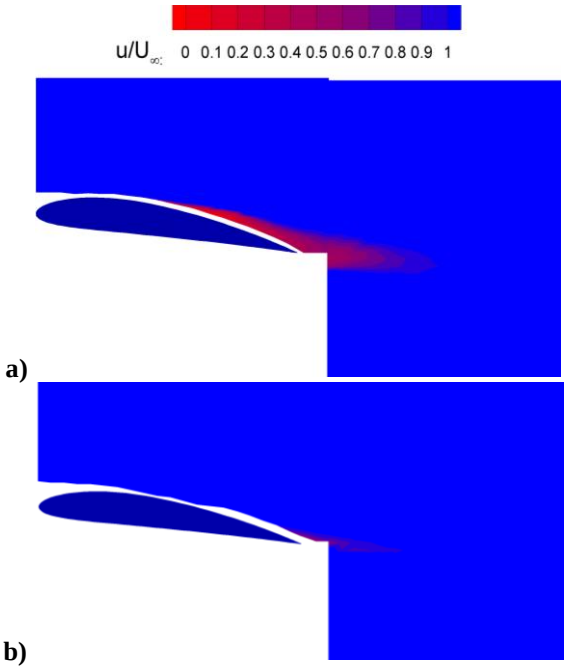

Fig. 6. Velocity measurements results for Re=5x10^4, α=8º and z/s=0.4 a) uncontrolled case, b) partial flexible airfoil.

Results of Reynolds stresses and turbulent intensity for both uncontrolled case and partially flexible airfoil are shown in Figure 7 and Figure 8, respectively. Different contour colours at both Reynolds stress and turbulent intensity indicate amount of fluctuations in the shear layer and flow-field. As seen in Figure 7(a) and Figure 8(a), fluctuations have increased at x/c=0.42, showing the transition to turbulence. As remarked at study of Koca et al. [9], vortex shedding driven by both LSB and trailing edge have especially played a dominant role between x/c=1.1 and x/c=1.25 (near wake of airfoil). This means that larger vortices having lower frequency

have occurred in this region, causing the drag forces to increase. On the other hand, transition point is x/c=0.39 when membrane material has been used over suction surface as a flow controller. That is, transition point has moved towards to leading edge. Unlike the uncontrolled case, fluctuations because of vortex sheds at near wake are less, meaning less drag force and steadier flow in terms of aerodynamic performance.

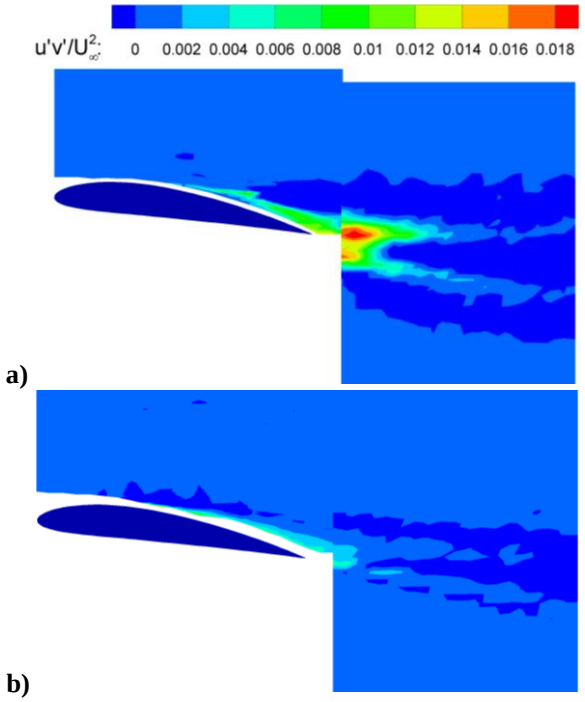

Fig. 7. Reynolds Stress results for Re=5x10^4, α=8º and z/s=0.4 a) uncontrolled case, b) partially flexible airfoil.

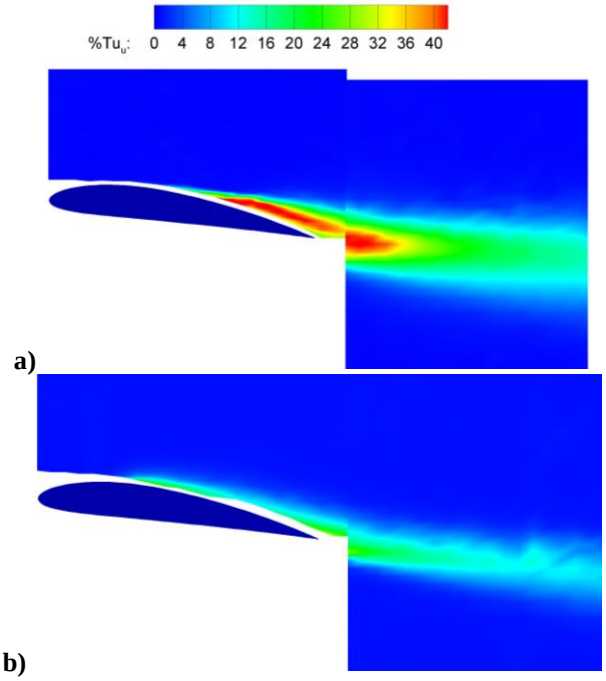

Fig. 8. Turbulence intensity results for Re=5x10^4, α=8º and z/s=0.4 a) uncontrolled case, b) partially flexible airfoil.

4 Conclusion

The objective of this experimental based study is to investigate the flow phenomena such as flow separation and LSB over suction surface of NACA 4412 airfoil with AR=1 at Re= 5x10^4 and different angles of attack. After flow investigation, flexible membrane material has been partially mounted between x/c=0.2 and x/c=0.7 to understand how membrane material has affected the flow characteristics under same flow condition. Smoke-wire experiment has been performed for z/c=0.1 and z/c=0.4 to observe LSB formation, flow separation and tip vortices at α=8º, α=12º α=20º. Additionally, hot-wire experiment have been employed to obtain velocity distributions, Turbulent intensity and averaged Reynolds stresses at α=8º. Results showed as follows:

- Smoke-wire results along z/c=0.4 indicated that along LSB have formed over suction surface of uncontrolled case between x/c=0.2 and x/c=0.8 at α=8º. Utilizing flexible membrane material over surface have obviously affected the flow characteristics especially by decreasing the size of LSB.

- Smoke-wire results along z/c=0.1 showed that increasing of angles of attack from α=12º to α=20º have led to improve the formation of tip-vortices throughout mid-span and wake region of uncontrolled case. For both angles of attack, tip-vortices have gradually been narrower especially at near wake region as partially flexible membrane material have been used, causing effect of drag forces to mitigate.

- Velocity distribution from hot-wire results demonstrated that LSB and flow separation have formed near at mid-span of uncontrolled case and α=8º because of APG, while these flow phenomena have suppressed by making the flow to reattaches to surface with use of flexible material.

- Finally, vortex sheds and amount of fluctuations obtained from turbulent statics including turbulent intensity and Reynolds stresses have illustrated that onset of transition have occurred at x/c=0.42 and α=8º and it has moved towards to leading-edge as flexible membrane has been used. Moreover, vortex sheds coming from both LSB and trailing-edge have played prevailing role on near wake region for the uncontrolled case, whilst mounting flexible material have restrained the power of fluctuations by doing damping effect, resulting in presence of narrower wake region (inherently meaning of lower drag forces).

References

1. Tani I., Prog Aerosp Sci, 5: 70–103, (1964).
2. Gaster, M. Aeronautical Research Council Reports and Memoranda, No: 3595, London, (1967).
3. T.J. Mueller, J.D. DeLaurier. Annual review of fluid mechanics, **35(1)**, 89-111 (2003)

4. M.S., Genç, I. Karasu, H.H. Açıkel, M.T., Akpolat. In Low Reynolds number aerodynamics and transition. InTech. (2012)
5. H. Demir, M. Özden, M.S. Genç, M. Çağdaş. In EPJ Web of Conferences (Vol. **114**, p. 02016). EDP Sciences, (2016)
6. M.S. Genç, K. Koca, H.H. Açıkel, G. Özkan, M.S. Kırış, R. Yıldız. In EPJ Web of Conferences (Vol. **114**, 2029 (2016)
7. M.S. Genç, G. Özkan, M. Özden, M.S. Kırış, R. Yıldız. Proc IMechE, Part C: Journal of Mechanical Engineering Science, **232(22)**, 4019-4037 (2018)
8. I. Karasu, M. Özden, M.S. Genç, Journal of Fluids Engineering-Transactions of The ASME, 140(12) 121102-1-121102-15 (2018).
9. K. Koca, M.S. Genç, H.H. Açıkel, M. Çağdaş, T.M. Bodur. Energy, **144**, 750-764 (2018)
10. H.H. Açıkel, M.S. Genç. Proceedings of the Institution of Mechanical Engineers, Part G: Journal of Aerospace Engineering, **230(13)**, 2447-2462 (2016).
11. M.S. Genç. H.H. Açıkel, M.T. Akpolat, G. Özkan, İ. Karasu, Journal of Aerospace Engineering-ASCE, 29 (6), 04016045, 2016.
12. M.S. Genç, Ü. Kaynak, G.D. Lock. Proc IMechE, Part G: Journal of Aerospace Engineering, **223(3)**, 217-231 (2009)
13. H. Wang, B. Zhang, Q. Qiu, X. Xu. Energy, **118**, 1210-1221 (2017)
14. K. Koca, M.S. Genç, H.H. Açıkel. Çukurova Üniversitesi Mühendislik-Mimarlık Fakültesi Dergisi, **31(ÖS2)**, 127-134 (2016)
15. M.S. Genç, K. Koca, H.H. Açıkel. Energy, **176**, 320-334 (2019)
16. W. Shvy, F. Klevebring, M. Nilsson, J. Sloan, B. Carroll, C. Fuentes. Journal of Aircraft, **36(3)**, 523-529 (1999)
17. Y. Lian, W. Shvy, D. Viieru, B. Zhang. Progress in Aerospace Sciences, **39(6-7)**, 425-465 (2003)
18. P. Rojratsirikul, M.S. Genç, Z. Wang, I. Gursul. Journal of Fluids and Structures, **27(8)**, 1296-1309 (2011)
19. H.H. Açıkel, M.S. Genç. Energy, **165**, 176-190 (2018)
20. Genç, M. S., Açikel, H. H., Demir, H., Özden, M., Çağdaş, M. and Isabekov, EPJ Web of Conferences. 114 02028 (2016).
21. Genç, M. S., Özden, M., Açikel, H. H., Demir, H. and Isabekov, EPJ Web of Conferences. 114, 02030 (2016).
22. Demir, H. and Genç, M. S. European Journal of Mechanics-B/Fluids, 65, 326-338 (2017).
23. Shyy, W., Berg, M. and Ljungqvist, D. Progress in aerospace sciences, 35(5), 455-505 (1999)..
24. Timpe, A., Zhang, Z., Hubner, J. and Ukeiley, L. Experiments in Fluids, 54(3), 1-23 (2013).
25. Genç, M. S. Experimental Thermal and Fluid Science, 44, 749-759 (2013).
26. Tregidgo L., Wang Z., Gursul I., Aerospace Science and Technology, Vol. 28, pp. 79-90, (2013).
27. Beguin B., Breitsamter C., Aerospace Science and Technology, 37, 138-150, (2014).
28. Alioli M., Masarati P., Morandini M., Albertani R., Carpenter T., Aerospace Science and Technology, 69, 419-431, (2017).
29. Nguyen A.T., Han J.H., Aerospace Science and Technology, 79, 468-481, (2018).
30. Ryu Y.G., Chang J.W., Chung J., Aerospace Science and Technology, 86, 558-571, (2019).
31. Bleischwitz, R., De Kat, R., & Ganapathisubramani, B. In 45th AIAA Fluid Dynamics Conf. 2764, (2015).
32. Hu, H., Kumar, A. G., Abate, G., & Albertani, R. Aerospace Science and Technology, 14(8), 575-586 (2010).